

## 論文

### ZrNi-H 系の磁気特性

赤丸悟士、岡崎圭祐、原 正憲、波多野雄治、松山政夫

富山大学水素同位体科学研究センター  
〒930-8555 富山市五福 3190

### Magnetic properties of ZrNi-H systems

Satoshi Akamaru, Keisuke Okazaki, Masanori Hara, Yuji Hatano,  
and Masao Matsuyama

Hydrogen Isotope Research Center, University of Toyama, Gofuku 3190,  
Toyama 930-8555, Japan

(Received December 20, 2013; Accepted May 23, 2014)

#### Abstract

We estimate the amount of hydrogen isotope gas stored in getter materials without using a desorption process and by measuring the magnetic susceptibility of ZrNi-H systems. The magnetic susceptibility of ZrNiH<sub>x</sub> increased with an increase in the hydrogen content,  $x$ , reaching a maximum value at  $x \cong 0.5$ . As  $x > 0.5$ , the magnetic susceptibility began to decrease and reached a minimum value at  $x = 2.7$ . The behavior of magnetic susceptibility could be qualitatively modeled using the molar fractions of the ZrNi, monohydride, and trihydride phases observed using X-ray diffraction analysis.

#### 1. Introduction

The hydrogen storage properties of a ZrNi getter, such as low equilibrium pressure, resistance to disproportion via hydrogen uptake, and relatively low desorbing temperatures are favorable for the safe storage and supply of hydrogen isotope gas [1].

Therefore, a ZrNi getter is one of the candidates for tritium storage getter in future nuclear fusion reactors [2-4].

Estimating the amount of tritium gas stored in a ZrNi getter is important for managing the tritium gas inventory. In general, this amount is estimated using a volumetric method: gas pressure and volume are measured after desorption of tritium gas from a ZrNi getter. In ordinary managements, estimating the stored tritium amount via desorption techniques is difficult because there is a possibility of tritium leakage during the measurement process. A calorimetric method is a reliable candidate for measuring the stored tritium amount without a desorption process. In this method, the amount of tritium is estimated based on the decay heat [5-12]. This method is advantageous over the volumetric method, but an accurate estimation with the calorimetric method requires a measurement time of ~24 h.

The magnetic properties of a getter material can be utilized to estimate the amount of hydrogen isotope gas stored in a getter without a desorption process; this is because the magnetic properties often depend on the amount of absorbing hydrogen isotope gas. For example, the magnetic susceptibility for the Pd-H systems is proportional to the amount of hydrogen in Pd [13]. The estimation method using the magnetic susceptibility of a getter has a few advantages over other methods: the measurement is performed with keeping hydrogen isotope gas in the getter, and the measurement time is short. Therefore, this method could be applicable to the regular monitoring of hydrogen isotopes stored in a getter material. To apply this method to a ZrNi getter, the magnetic properties of ZrNi-H systems should be investigated.

In this work, the dependence of the magnetic susceptibility on the stored hydrogen amount in a ZrNi getter at room temperature was investigated. In addition, the behavior

of the magnetic susceptibility relative to the stored hydrogen amount was discussed based on the molar fractions of the crystallographic phases formed in ZrNi-H systems.

## 2. Experimental

Zr and Ni grains, the initial materials used for preparing a ZrNi getter, were purchased from Furuuchi Chemical Co. Ltd. and Kojyundo Kagaku K.K., respectively. The purities were 99.7% and 99.9% for Zr and Ni, respectively. The grains were weighed to yield an atomic ratio of 1:1, and they were then compounded into a ZrNi ingot by using an arc furnace under argon atmosphere. To remove residual oxygen in the argon atmosphere, a titanium ingot was melted in advance. The ZrNi powder was obtained using the following process: the ZrNi ingot was cut into cubes  $\sim 10 \times 10 \times 10 \text{ mm}^3$ , and the cubes were inserted into a quartz cell attached to a vacuum system. The cell was set at  $5 \times 10^{-5} \text{ Pa}$ , and a heat treatment at a temperature of 873 K was then performed as an activation process. Hydrogen gas at a pressure of  $10^5 \text{ Pa}$  was introduced into the cell at room temperature. Because the hydrogen gas pressure gradually decreased with hydrogen uptake, hydrogen gas was repetitively added to maintain the gas pressure. After a week, the ZrNi ingot was completely pulverized from the hydrogen uptake. The ZrNi hydride powder was taken out to air, and  $\sim 0.25 \text{ g}$  of the powder was transferred to a quartz measurement cell. The measurement cell was evacuated to  $5 \times 10^{-5} \text{ Pa}$ , followed by the annealing of the cell with the ZrNi powder at 873 K for 3 h to completely desorb hydrogen from the ZrNi hydride.

The magnetic susceptibility and amount of hydrogen stored in the ZrNi powder were measured by a self-made, pressure-composition isotherm measurement system equipped with an alternative magnetic susceptibility measurement system. The details of the

system were already described in a previous paper [13]. The measurement process was as follows: hydrogen gas at a certain pressure was exposed to the ZrNi powder, and the pressure decreased with hydrogen uptake. Once the pressure became constant, the hydrogen pressure in the gas phase and stored hydrogen amount had reached equilibrium. The hydrogen content at equilibrium, which corresponds to the stored hydrogen amount in the ZrNi powder, was calculated based on the pressure drop. Next, the alternating magnetic susceptibility at equilibrium was measured. This process was repeated until the equilibrium pressure reached  $\sim 100$  kPa. All measurements were performed at room temperature. X-ray diffraction (XRD) patterns were measured using the X'pert system (Panalytical) using Cu-K $\alpha$  x-rays. The acceleration voltage was 40 kV, and the range of the diffraction angle was  $25^\circ$ – $50^\circ$ .

### 3. Results and discussion

Figure 1 shows the dependence of magnetic susceptibility on the hydrogen content for the ZrNi–H systems at room temperature. The magnetic susceptibility of ZrNi powder without hydrogen was  $22.0 \times 10^{-9} \text{ m}^3/\text{kg}$ , which agreed with previously reported data [14]. The magnetic susceptibility gradually increases with increasing hydrogen content and has a maximum value of  $23.1 \times 10^{-9} \text{ m}^3/\text{kg}$  at a hydrogen content of  $\sim 0.5$ . For the

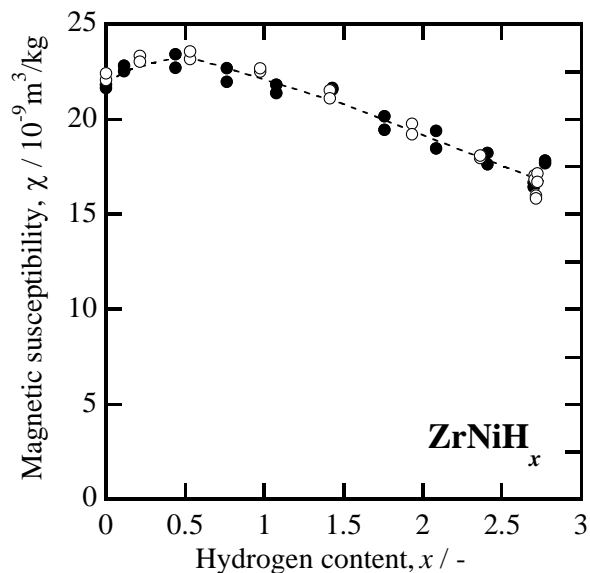


**Figure 1.** Magnetic susceptibilities of the ZrNi–H systems at room temperature. The open and closed symbols indicate corresponding results obtained in the first and second cycles of measurements.

hydrogen content above 0.5, the magnetic susceptibility decreased linearly with increasing hydrogen content. In this study, the ZrNiH<sub>2.7</sub> system with the maximum hydrogen content has a minimum magnetic susceptibility of  $16.6 \times 10^{-9}$  m<sup>3</sup>/kg. To confirm the reproducibility of the magnetic susceptibility dependence on the hydrogen content, the magnetic susceptibility for the ZrNi–H systems was measured as a function of hydrogen content the second time after the desorption of all the hydrogen absorbed in the first cycle of the measurement (Fig. 1). Results obtained in the second cycle of measurement were consistent with those from the first cycle, indicating the magnetic susceptibility values to be quantitatively reproducible.

The peak structure in the magnetic susceptibility is possibly because of changes in the crystallographic phases upon hydrogen uptake. ZrNi hydride is characterized by two crystallographic phases, namely monohydride and trihydride phases [15]. The pressure composition isotherm reported previously [16] indicated that the ZrNi and monohydride phases coexist at the hydrogen contents lower than 1.0, and the monohydride and trihydride phases coexist in the hydrogen content range between 1.0 and 2.7.

To confirm changes in the crystallographic phase of the ZrNi–H systems based on hydrogen content, four samples with different hydrogen contents were prepared, and the XRD measurements of these samples were performed. Figure 2 shows the XRD patterns of the ZrNiH<sub>0.0</sub>, ZrNiH<sub>0.5</sub>, ZrNiH<sub>1.0</sub>, and ZrNiH<sub>2.7</sub> systems (ZrNi hydride with hydrogen content in the ratio  $[H]/[ZrNi] = x$  is denoted as ZrNiH<sub>x</sub>).

The XRD pattern of the ZrNiH<sub>0.0</sub> system clearly shows peaks related to the ZrNi phase. A minor peak related to the trihydride phase is also observed, and the appearance of this peak can be explained by the capture of residual hydrogen during pulverization of the ZrNi ingot.

New peaks related to the monohydride phase clearly appear in the XRD pattern of the  $\text{ZrNiH}_{0.5}$  system, indicating that this system is composed of  $\text{ZrNi}$  and monohydride phases. The  $\text{ZrNiH}_{1.0}$  system is also mainly composed of the  $\text{ZrNi}$  and monohydride phases, and in addition to this, the trihydride phase appears to have grown. The XRD pattern of the  $\text{ZrNiH}_{2.7}$  system shows only the trihydride phase. These results reveal that the crystallographic phases of  $\text{ZrNi-H}$  systems change with hydrogen uptake.

XRD measurements also point out that the molar fraction of each phase in the  $\text{ZrNi-H}$  system also changed with hydrogen uptake because the relative peak intensity between these three phases changed in the four samples.

We attempted to estimate the molar fraction for the three phases by calculating the peak area of each phase in the XRD patterns. The peak areas of the selected peaks corresponding to each phase (the selected peaks are indicated by

gray areas in Figure 2) can be calculated using peaks reproduced by a Gaussian function.

The molar fraction of the  $\text{ZrNi}$ , monohydride, and trihydride phases in each sample was determined using the following method. The  $\text{ZrNiH}_{2.7}$  system only comprises the

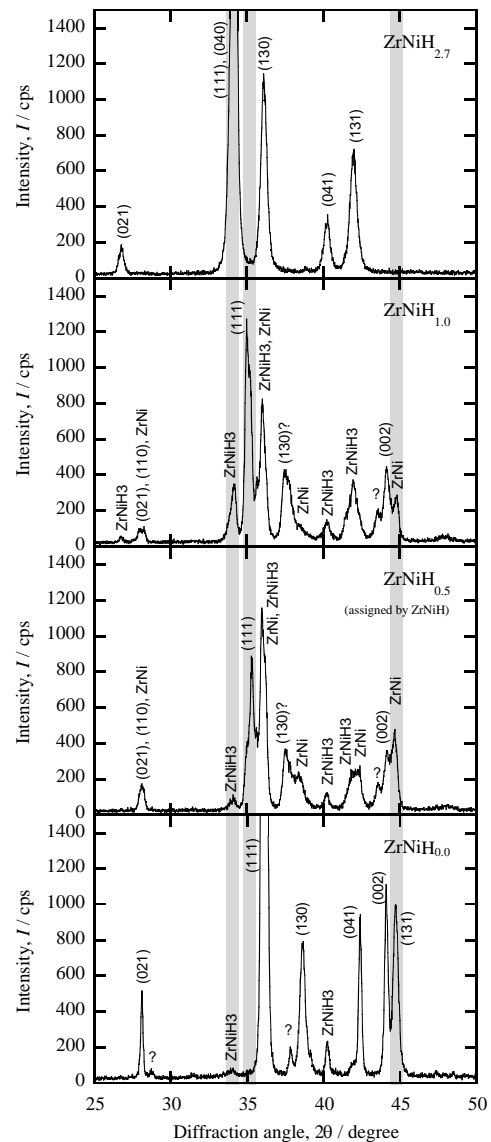


**Figure 2.** XRD patterns of four  $\text{ZrNi}$  hydrides with different hydrogen content. The gray areas indicate the analyzed peaks of the molar fractions shown in Figure 3; the gray areas around  $34^\circ$ ,  $35^\circ$ , and  $45^\circ$  correspond to the (040) and (111) peaks related to the trihydride phase, the (111) peak related to the monohydride phase, and the (131) peak related to the  $\text{ZrNi}$  phase, respectively.

trihydride phase, and the sums of the (111) and (040) peak areas related to the trihydride phase in each sample were normalized assuming that the molar fraction of the trihydride phase,  $C_{\text{tri}}$ , in the  $\text{ZrNiH}_{2.7}$  system was 100%. Because the  $\text{ZrNiH}_{0.0}$  system comprises the ZrNi and trihydride phases, the molar fraction of the ZrNi phase in this system was determined by the subtraction of the trihydride phase fraction; the result was 99%. The molar fractions of the ZrNi phase,  $C_{\text{ZrNi}}$ , in  $\text{ZrNiH}_{0.5}$  and  $\text{ZrNiH}_{1.0}$  systems were determined by comparing the corresponding ZrNi (131) peak areas with the ZrNi peak area for the  $\text{ZrNiH}_{0.0}$  system, and they were 41% and 24% for  $\text{ZrNiH}_{0.5}$  and  $\text{ZrNiH}_{1.0}$ , respectively. Finally, the molar fractions of the monohydride phase,  $C_{\text{mono}}$ , in the  $\text{ZrNiH}_{0.5}$  and  $\text{ZrNiH}_{1.0}$  systems were determined by subtracting the fractions of the ZrNi and trihydride phases, and they were 57% and 66% for  $\text{ZrNiH}_{0.5}$  and  $\text{ZrNiH}_{1.0}$ , respectively. The molar fractions of the ZrNi, monohydride, and trihydride phases for

each sample are plotted in Figure 3. The amount of hydrogen stored in each sample can therefore be calculated based on the phase fraction (Figure 3). These results are summarized in Table I. The calculated hydrogen contents in each sample are almost consistent with the actual hydrogen contents, proving that the phase fractions can be well estimated from the XRD patterns.

The magnetic susceptibility of these four samples can be estimated using the molar fractions (Figure 3). First, the magnetic susceptibility of each single phase was determined. Because the  $\text{ZrNiH}_{2.7}$  system comprises a single trihydride phase, the

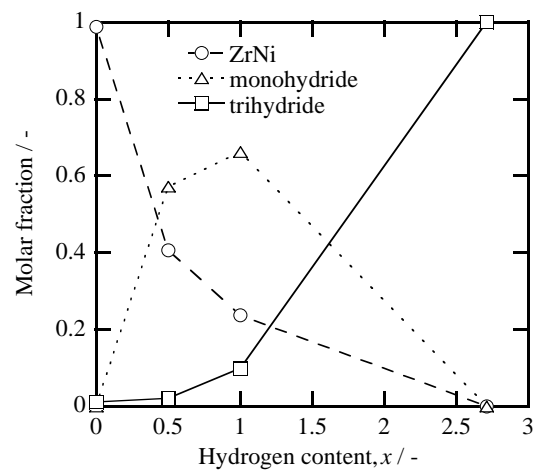


**Figure 3.** The estimated molar fraction of each phase using the typical X-ray diffraction peaks for each phase as indicated in Figure 2.

**Table I.** The calculated hydrogen content and magnetic susceptibility for each ZrNi-H system. The magnetic susceptibility of the ZrNi phase is estimated to be  $22.1 \times 10^{-9} \text{ m}^3/\text{kg}$  and that of the monohydride phase is assumed to be  $23.1 \times 10^{-9} \text{ m}^3/\text{kg}$ .

	Calculated hydrogen content	Magnetic susceptibility / $10^{-9} \text{ m}^3 \text{ kg}^{-1}$	
		$\chi_{\text{cal}}$	Measured value
ZrNiH <sub>0.0</sub>	0.03	22.0	22.0
ZrNiH <sub>0.5</sub>	0.63	22.4	23.1
ZrNiH <sub>1.0</sub>	0.93	22.1	22.1
ZrNiH <sub>2.7</sub>	2.71	16.6	16.6

magnetic susceptibility of the ZrNiH<sub>2.7</sub> system, measured as  $16.6 \times 10^{-9} \text{ m}^3/\text{kg}$ , can be assigned to the trihydride phase,  $\chi_{\text{tri}}$ . The ZrNiH<sub>0.0</sub> system includes a small amount of the trihydride phase; therefore, the magnetic susceptibility of the ZrNi phase,  $\chi_{\text{ZrNi}}$ , is slightly larger than that of the ZrNiH<sub>0.0</sub> system and is estimated to be  $22.1 \times 10^{-9} \text{ m}^3/\text{kg}$ . Because the magnetic susceptibility of the ZrNi-H systems has a maximum at a hydrogen content of  $\sim 0.5$  (Figure 1), the magnetic susceptibility of the monohydride phase is expected to be larger than that of the ZrNi phase. We assume the magnetic susceptibility of the monohydride phase,  $\chi_{\text{mono}}$ , to be  $23.1 \times 10^{-9} \text{ m}^3/\text{kg}$ . The total magnetic susceptibility,  $\chi_{\text{cal}}$ , of each system was calculated as;

$$\chi_{\text{cal}} = C_{\text{ZrNi}} \chi_{\text{ZrNi}} + C_{\text{mono}} \chi_{\text{mono}} + C_{\text{tri}} \chi_{\text{tri}}.$$

The  $\chi_{\text{cal}}$  values for the four ZrNi-H systems are summarized in Table I. The  $\chi_{\text{cal}}$  values are almost the same as the experimentally measured values for the magnetic susceptibility, indicating that the magnetic susceptibilities for the ZrNi-H systems can be qualitatively understood based on the molar fraction of the ZrNi, monohydride, and trihydride phases. Notably, the  $\chi_{\text{cal}}$  of the ZrNiH<sub>0.5</sub> system is smaller than the one measured. This is mainly because of the uncertain molar fraction estimated from the XRD patterns. More accurate determination of the fractions of these three phases in each sample will be required to quantitatively determine the magnetic susceptibility.



#### 4. Conclusions

The magnetic susceptibilities for ZrNi-H systems with various hydrogen contents were measured at room temperature. The magnetic susceptibility reached a maximum at a hydrogen content of  $\sim 0.5$ , and monotonically decreased with an increase in the hydrogen content above 0.5. The XRD measurements of four samples with different hydrogen content indicated that several phases coexist in the samples. For example, the ZrNiH<sub>1.0</sub> system is composed of three phases: the ZrNi, monohydride, and trihydride phase.

The behavior of magnetic susceptibility in ZrNi-H systems could be qualitatively modeled using the molar fractions of the ZrNi, monohydride, and trihydride phases observed by X-ray diffraction analysis. The molar fraction of each phase can be estimated using the area of the diffraction peak assigned to this phase. The magnetic susceptibility of each phase can be qualitatively determined by knowing the experimentally measured magnetic susceptibilities and phase fractions for each ZrNi-H system.

For the ZrNi-H systems, the magnetic susceptibility measurements can be used to estimate the amount of hydrogen stored in the ZrNi getter at higher hydrogen contents (above 0.5). To estimate the amount of hydrogen stored in a ZrNi getter at lower hydrogen contents, suppressing the growth of the monohydride phase by alloying, i.e., Zr(Ni<sub>1-x</sub>Co<sub>x</sub>) is necessary.

#### Acknowledgement

This study was supported by Grant-in-Aid for Scientific Research on Prior Areas, Tritium for Fusion (No 476) from MEXT, Japan.

## References

- [1] G. G. Libowitz, H. F. Hayes, T. R. P. Gibb, Jr., *Journal of Physical Chemistry* **62** (1958) 76-79.
- [2] K. Watanabe, K. Tanaka, M. Matsuyama, K. Hasegawa, *Fusion Engineering and Design* **18** (1991) 27-32.
- [3] T. Kabutomori, Y. Wakisaka, K. Tsuchiya, H. Kawamura, *Journal of Nuclear Materials* **258-263** (1998) 481-487.
- [4] K. Tsuchiya, T. Kabutomori, H. Kawamura, *Fusion Engineering and Design* **58-59** (2001) 401-405.
- [5] J. L. Hemmerich, *Fusion Technology* **28** (1995) 1732-1736.
- [6] A. Perevezentsev and J. Hemmerich, *Fusion Science and Technology* **41** (2002) 797-800.
- [7] J. E. Klein, M. K. Mallory, and A. Nobile, Jr., *Fusion Technology* **21** (1992) 401-405.
- [8] T. Hayashi, T. Suzuki, M. Yamada, and M. Nishi, *Fusion Technology* **34** (1998) 510-514.
- [9] T. Hayashi, M. Yamada, T. Suzuki, Y. Matsuda, and K. Okuno, *Fusion Technology* **28** (1995) 1015-1019.
- [10] T. Hayashi, T. Suzuki, M. Yamada, and K. Okuno, *Fusion Technology* **30** (1996) 931-935.
- [11] T. Hayashi, T. Suzuki, M. Yamada, and M. Nishi, *Fusion Science and Technology* **48** (2005) 317-323.
- [12] S O'hira, T. Hayashi, H. Nakamura, K. Kobayashi, T. Tadokoro, H. Nakamura, T. Itoh, T. Yamanishi, Y. Kawamura, Y. Iwai, T. Arita, T. Maruyama, T. Kakuta, S. Konishi,

M. Enoeda, M. Yamada, T. Suzuki, M. Nishi, T. Nagashima, and M. Ohta, *Nuclear Fusion* **40** (2000) 519-525.

[13] S. Akamaru, M. Hara, and M. Matsuyama, *Review of Scientific Instruments* **83** (2012) 075102.

[14] E. M. Carvalho and I. R. Harris, *Journal of Less Common Metals* **106** (1985) 117-128.

[15] D. G. Westlake, *Journal of the Less Common metals* **75** (1980) 177-185.

[16] R. Kronski and T. Schober, *Journal of Alloys and Compounds* **205** (1994) 175-178.